ISSN 2278-2540 | DOI: 10.51583/IJLTEMAS | Volume XV, Issue V, May 2026

Effect of calcination temperature on biodiesel production from palm kernel oil using a bifunctional catalyst derived from calcium carbide residue (CCR) and anthill clay (AC)

Justina Oduwa Okhonmina[1]* and Kessington Obahiagbon[2]

[1,2]Department of Chemical Engineering, Faculty of Engineering, University, of Benin, Benin City, Edo State, Nigeria.

DOI: https://doi.org/10.51583/IJLTEMAS.2026.150500239

Received: 25 May 2026; Accepted: 30 May 2026; Published: 19 June 2026

ABSTRACT

This study aims at investigating the effect of calcination temperature on biodiesel production from palm kernel oil using a bifunctional catalyst derived from calcium carbide residue (CCR) and anthill clay (AC). The specific objectives include to synthesize a ZnO-doped CaO/Anthill clay composite using CCR and anthill clay as precursors, to evaluate the effect of various calcination temperatures (650 **°C** to 850 **°C**) on the catalyst's chemical and structural properties, to identify the optimal temperature that maximizes the density of active sites while preventing structural degradation, and to test the catalyst's effectiveness by converting palm kernel oil (PKO) into biodiesel and evaluating the final yield. The CCR and AC precursors were prepared and characterized using X-ray diffraction, scanning electron microscopy, Fourier Transform Infrared spectroscopy, X-ray fluorescence, and Brunauer-Emmett-Teller. Composites of the prepared CCR and AC were formulated in ratios 1:4, 2:3, 1:1, 3:2, and 4:1 of CCR:AC and doped with 1.5 M zinc nitrate, by wet impregnation and calcined at 3 different temperatures (650 ^{o}C, 750 ^{o}C, and 850 ^{o}C), resulting in 15 samples (A1 – E3) which were used for the production. Ratio 2:3 catalyst (D2) calcined at 750 ^{o}C gave the highest yield (92.73%) and reusability studies gave an overall reduction of 27.69 % in yield across 6 cycles. Its XRF analysis gave compositions of 52.1% CAO, 10.4% SiO_2, and 7.4% Al_2O_3. Its surface area, pore diameter and pore volume were 226.9m^2/g, 2.9nm and 0.2cc/g respectively. The PKO characterization results showed the PKO's suitability for the biodiesel production. The produced biodiesel properties aligned with ASTM D6571 and EN 14214 standards upon characterization. This study successfully synthesized a high-performance ZnO-doped CaO/Anthill clay composite from sustainable materials, identifying calcination temperature as the key factor influencing catalyst activation and structural stability and also contributes to the promotion of renewable and sustainable energy.

Keywords: Palm kernel oil, Calcium Carbide Residue, Anthill clay, Calcination Temperature, Biodiesel.

INTRODUCTION

The global shift toward sustainable energy has positioned biodiesel as a viable, carbon-neutral alternative to traditional fossil fuels. Biodiesel is an alternate energy source which is made from biological components like vegetable or animal fats and used cooking oils [17]. Transesterification is the most widely used technique for producing biodiesel [12]. It involves the reaction of triglycerides with alcohol (often methanol or ethanol) in the presence of a catalyst to produce glycerol and biodiesel [4]; [6]; [8]. While biodiesel offers lower emissions and high biodegradability, its commercial production is often limited by high costs. Homogeneous catalysts are largely responsible for this, as they cannot be recovered and require expensive water-washing steps. To overcome these barriers, recent research has focused on the "circular economy" by developing heterogeneous catalysts from industrial and environmental waste, such as calcium carbide residue (CCR) and anthill clay [11]; [17]; [19]. When heterogeneous catalysts are used in transesterification, they yield glycerin with greater purity and lower levels of dissolved ions [15].

ISSN 2278-2540 | DOI: 10.51583/IJLTEMAS | Volume XV, Issue V, May 2026

The performance of these waste-derived catalysts depends heavily on the calcination temperature. This thermal treatment is necessary to convert inactive mineral precursors into reactive oxides like CaO and ZnO. However, finding the optimal temperature is a major challenge. If the temperature is too low, the catalyst remains chemically inactive; if it is too high, the material undergoes sintering, which causes the internal pores to collapse and reduces the surface area available for the reaction [2]; [14]. Identifying the precise thermal "sweet spot" is therefore essential for creating an efficient and stable catalyst.

MATERIALS & METHODS

Collection of materials

The CCR and AC precursors were obtained from some welder's shop and anthill respectively, in Ugbowo in Benin City, Edo State, Nigeria. The PKO was purchased from a local vendor in Benin City also.

Catalyst preparation

According to Okhonmina et al. [17], the locally sourced precursors were beneficiated, pulverized and screened to < 200µm and calcined at 800 ^{o}C for 4 hours. The calcined AC was treated with 2M H_2SO_4, washed and dried. It was calcined again at 800 ^{o}C for 2 hours, 30 minutes. The precursors were combined in 5 different ratios; 1:4, 2:3, 1:1, 3:2, and 4:1 of CCR:AC. The samples were then doped with equal quantities of 1.5 M zinc nitrate at a composite material-to-zinc nitrate ratio of 1:4 using the wet impregnation technique to produce suspensions. These suspensions were continuously stirred on a magnetic stirrer at 80 °C for 6 h to ensure proper homogenization. Thereafter, the mixtures were left to settle, and the excess liquid was removed through decantation. The resulting slurries were dried in a vacuum oven at 120 °C until complete dehydration was achieved. The dried doped composite materials, prepared in five different proportions, were subsequently pulverized and sieved to obtain particle sizes below 200 µm. Each composite sample was then divided into three portions and calcined in a muffle furnace at 650 °C, 750 °C, and 850 °C under static air conditions for 4 hrs, resulting in 15 different catalyst samples (A1 – E3) which were used for the biodiesel production.

Catalyst characterization

The precursors and formulated catalyst were characterized using X-ray diffraction (XRD) analysis for crystalline phase, Scanning electron microscopy (SEM) with Energy Dispersive X-ray (EDX) for the surface structure, Fourier transform infrared spectroscopy (FTIR) for bond structure and interaction, X-ray fluorescence (XRF) analysis for elemental composition, and Brunauer-Emmett-Teller (BET) analysis for surface area and pore properties.

Characterization of palm kernel oil

The palm kernel oil was characterized to determine its suitability as feedstock for biodiesel production.

Production of biodiesel

Production of biodiesel was carried out using the 15 different catalysts at fixed input parameters of 65 ^{o}C, 90 mins, 9:1 and 3 wt % reaction temperature, reaction time, methanol to oil ratio and catalyst loading respectively. A one-step technique transesterification process was used for the biodiesel production, based on the bi-functionality of the synthesized catalyst. A batch-type stirred reactor which comprised a hot plate magnetic stirrer with a magnetic stirring bar for proper mixing to obtain uniform mixture, and a 250ml conical flask with a cork was employed for the biodiesel production. 50g of the PKO was transferred into the reactor and heated to 65 ^{o}C. 3 wt % of catalyst and 9:1 methanol to oil ratio mixture was added, and the mixture was left to react for 90 mins [17], using a fixed stirring speed.

After each production, the resulting mixture was transferred into a separating funnel and left to stay overnight for proper settling, after which the glycerol at the bottom layer was run out with the aid of the separating funnel.

ISSN 2278-2540 | DOI: 10.51583/IJLTEMAS | Volume XV, Issue V, May 2026

The biodiesel with the unreacted methanol mixture was washed and transferred to an oven. The unreacted methanol evaporated while the biodiesel was stored. The transesterification process, separation process and the produced PKO biodiesel are displayed below in figure 1 (a), (b) and (c) respectively. Equation 1 below was used to determine the biodiesel yield.

$$biodiesel\ yield\ (\%) = \frac{(weight\ of\ biodiesel\ produced)}{(weight\ of\ PKO\ used)} \times 100 \quad (1)$$

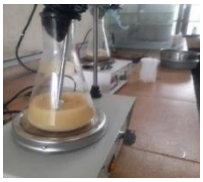

(a) (b) (c)

Figure 1: Biodiesel production process (a) transesterification process (b) separation process (c) produced PKO biodiesel

All experiments were conducted in triplicate to ensure the reliability and reproducibility of the results, and the average values obtained were reported. Furthermore, the reaction conditions were carefully controlled throughout the experimental process to minimize errors and maintain consistency in the biodiesel production procedure.

Catalyst reusability studies

The reusability of the catalyst that gave the highest yield was evaluated through repeated transesterification reactions under optimum conditions. After each cycle, the catalyst was recovered by filtration, washed with methanol, and oven-dried at 80 °C for 12 hours before reuse. The recovered catalyst was reused for six consecutive cycles, and the biodiesel yield obtained after each run was recorded.

Characterization of the produced biodiesel

The produced biodiesel was characterized to determine its properties such as acid value, FFA, saponification value, average molecular weight, density, kinematic viscosity, moisture content, iodine value, peroxide value, etc.

RESULTS AND DISCUSSION

X-ray diffraction (XRD) analysis

With the aid of the XRD analysis, identification of the crystalline phases was achieved and the structure and physical properties of the precursors and composite catalyst were determined [18]. Figure 2 (a), (b) and (c) below show the XRD pattern of the precursors and composite catalyst.

The XRD pattern of the calcined calcium carbide residue (CCR) precursor in figure 2 (a) reflects the complete thermal transformation of its original carbonate and hydroxide phases. The pretreatment at 800 °C ensures the full decomposition of Portlandite [$Ca(OH)_2$] and Calcite [$CaCO_3$] into cubic calcium oxide (CaO). This is evidenced by sharp, high-intensity diffraction peaks at 2θ values of approximately 32.2°, 37.4°, and 53.9° [14]. The high degree of crystallinity at this temperature provides a stable source of basic active sites, which are essential for the subsequent transesterification of triglycerides [13].

The diffraction pattern of the anthill clay (AC) precursor in figure 2 (b), also calcined at 800 °C, indicates a structural shift toward a more reactive aluminosilicate state. The thermal energy at this level facilitates the transition of Kaolinite into metakaolinite, characterized by the disappearance of kaolinite reflections and the

ISSN 2278-2540 | DOI: 10.51583/IJLTEMAS | Volume XV, Issue V, May 2026

presence of a broad amorphous halo between 2 θ = 20° and 30° [22]. The persistent sharp peak at 26.6° signifies the stable crystalline Quartz (SiO_2) fraction of the clay. This combination of a stable crystalline framework and a reactive amorphous phase provides the necessary acidic sites and structural support for the composite material.

The XRD pattern of the final composite catalyst in figure 2 (c) —prepared at a 3:2 ratio of CCR to AC and calcined at 750 °C—demonstrates the successful integration of the 1.5 M zinc nitrate dopant into the precursor matrix. This pattern is characterized by the co-existence of sharp reflections for cubic CaO and hexagonal wurtzite ZnO, with the latter appearing at 2 θ values of 31.8°, 34.4°, and 36.2° [3]. The secondary calcination at 750 °C serves as the critical activation stage for the doped zinc species, ensuring they are well-dispersed across the aluminosilicate surface of the anthill clay and the basic surface of the CaO.

The presence of distinct CaO and ZnO peaks confirms the bifunctional nature of the catalyst. The basic sites provided by the CCR-derived CaO and the acidic sites provided by the ZnO and AC framework work in synergy to facilitate both transesterification and esterification. This 3:2 composition and 750 °C calcination temperature avoid the structural sintering often observed at 850 °C, maintaining a high active surface area. This structural arrangement is responsible for the peak biodiesel yield of 92.73%, as it provides the optimal electronic environment for methanol activation and free fatty acid conversion [16].

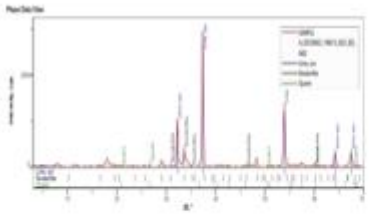

Figure 2(a): XRD pattern of CCR precursor

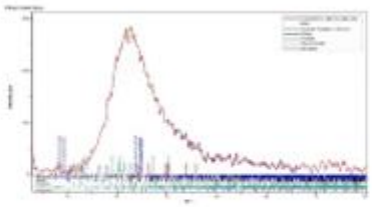

Figure 2(b): XRD pattern of AC precursor

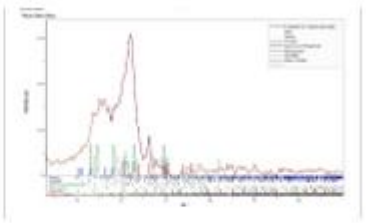

Figure 2(c): XRD pattern of composite catalyst

Scanning electron microscopy (SEM) with Energy Dispersive X-ray (EDX)

The surface morphology of the precursors and composite catalyst were observed using SEM. The results obtained at different magnifications are displayed below in figures 3, 4 and 5.

The calcined calcium carbide residue (CCR) (Figure 3) displays a highly agglomerated and irregular morphology. The 800 °C pretreatment promotes the formation of dense crystalline clusters, providing a robust source of basic active sites essential for initiating the transesterification process. The utilization of waste-derived precursors for catalyst synthesis not only reduces production costs but also promotes environmental sustainability by repurposing industrial byproducts. This approach is supported by Makarevičienė et al. [11], who demonstrated that properly prepared catalysts from natural waste and industrial residues exhibit superior catalytic properties for commercial-grade biodiesel conversion.

The anthill clay (AC) (Figure 4) exhibits a contrasting flaky and layered architecture. This sheet-like arrangement, typical of thermally treated aluminosilicates, provides a porous structural scaffold. This morphology is critical for enhancing the surface-area-to-volume ratio and facilitating the anchoring of metal oxide dopant [22].

The composite catalyst (Figure 5) reveals a significant transition toward a more granular and textured surface after 1.5 M zinc nitrate doping and 750 °C calcination. The images show a uniform distribution of active nanoparticles across the aluminosilicate flakes, creating an interconnected network of micro-pores. This morphology minimizes mass transfer resistance, allowing large triglyceride molecules to easily access active sites, which justifies the observed peak yield of 92.73% [20]. The absence of severe particle fusion suggests that the 750 °C treatment successfully optimized the catalyst's crystallinity without triggering the sintering-induced structural collapse often observed at higher temperatures [10].

ISSN 2278-2540 | DOI: 10.51583/IJLTEMAS | Volume XV, Issue V, May 2026

Figure 3: SEM images of CCR precursor (a) x340 (b) x500

Figure 4: SEM images of THC precursor (a) x500 (b) x1000

Figure 5: SEM images of composite catalyst (a) x500 (b) x750

Fourier transform infrared (FTIR) spectroscopy analysis

The identification of different functional groups available on the precursors and composite catalyst surfaces was carried out using Fourier transform infrared (FTIR) analysis. Figures 6 to 8 show the FTIR results of the precursors and composite catalyst.

The spectrum of the calcined CCR (Figure 6) shows a significant reduction in the O–H band (3640 cm^{-1}), indicating the dehydration of calcium hydroxide into Calcium Oxide (CaO). The remaining peaks at approximately 1420 cm^{-1} and 875 cm^{-1} are attributed to the stretching and bending vibrations of C–O bonds from atmospheric CO_2 adsorption on the basic CaO surface, confirming its high chemical reactivity [14].

The calcined anthill clay (AC) spectrum (Figure 7) reflects the thermal transition of kaolinite into metakaolinite. The loss of structural hydroxyl groups at 3695 cm^{-1} and 3620 cm^{-1} indicates successful dehydroxylation. The dominant band shifting toward 1050-1080 cm^{-1} represents the reactive amorphous Si–O–Al framework, while persistent peaks at 798 cm^{-1} confirm the stable Quartz fraction [22].

The composite catalyst (Figure 8), subsequently calcined at 750 °C, demonstrates the successful chemical integration of the 1.5 M zinc nitrate dopant. The spectrum is characterized by a broad, intense absorption band in the 400-600 cm^{-1} range, which is the direct result of metal-oxygen (M–O) vibrations for both Zn–O and Ca–O. This overlap confirms the formation of an integrated metal-oxide-aluminosilicate matrix. The presence of these combined functional groups validates the bifunctional nature of the catalyst, providing the acidic and basic sites necessary for the high biodiesel yield achieved in the production phase [2]; [11].

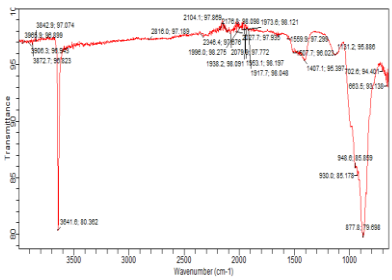

Figure 6: FTIR spectra of CCR precursor

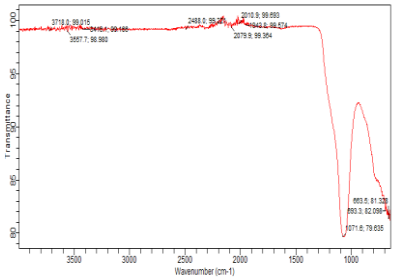

Figure 7: FTIR spectra of AC precursor

ISSN 2278-2540 | DOI: 10.51583/IJLTEMAS | Volume XV, Issue V, May 2026

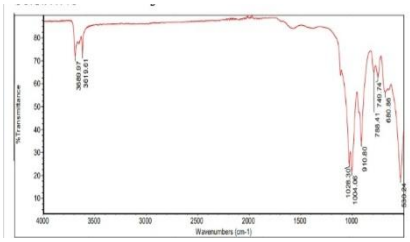

Figure 8: FTIR spectra of the composite catalyst

X-ray Fluorescence (XRF) Analysis

The elemental composition of the calcium carbide residue (CCR), anthill clay (AC), and the resulting composite catalyst reveals a strategic combination of active components and structural supports. The CCR precursor is highly rich in CaO (89.8%), establishing it as the primary source of basic active sites essential for the transesterification reaction [1]; [9]. The AC precursor contains significant amounts of SiO_2 (46.9%) and Al_2O_3 (24.1%), characteristic of aluminosilicate clays that serve as stable, high-surface-area frameworks for catalyst immobilization [5]; [21].

A significant chemical transformation is observed in the composite catalyst, specifically the inclusion of ZnO (20.9%), which was not present in substantial quantities in either precursor. This

enrichment indicates the successful introduction of a zinc-based dopant during synthesis to enhance the catalyst's bifunctionality and thermal stability [7]. The final composition effectively balances basicity from CaO (52.1%) with structural integrity and acidic sites provided by SiO_2, Al_2O_3, and ZnO, which is a hallmark of high-performance heterogeneous catalysts capable of achieving biodiesel yields above 90% [1]; [7]. Table 1 shows the elemental composition of CCR precursor, AC precursor and the composite catalyst.

Table 1: Elemental composition of CCR precursor, AC precursor and composite catalyst

Component	**CCR precursor**	**AC precursor**	**Concentration (%) of composite catalyst**
CaO	89.8	1.5	52.1
SiO_2	4.04	46.9	10.4
Al_2O_3	3.9	24.1	7.4
SO_3	0.6	0.4	0.3
Fe_2O_3	0. 4	20.6	5.2
Cl	0. 43	0.7	0.9
SnO_2	0. 25	0.0	0.3
TiO_2	0.13	3.8	0.9
CoO	0.09	0.1	0.02
BaO	0.09	0.0	0.02
SrO	0.06	0.02	0.06
CuO	0.06	0.14	0.05
Ta_2O_5	0.05	0.06	0.2
ZrO_2	0.03	0.5	0.3
Cr_2O_3	0.03	0.1	0.03

ISSN 2278-2540 | DOI: 10.51583/IJLTEMAS | Volume XV, Issue V, May 2026

WO_3	0.02	0.0	0.5
NiO	0.02	0.01	0.0
PbO	0.01	0.04	0.03
V_2O_5	0.01	0.2	0.07
MnO	0.01	0.1	0.04
Cs_2O	0.01	0.09	0.08
ZnO	0.01	0.04	20.9
Rb_2O	0.00	0.01	0.01
Nb_2O_5	0.0	0.04	0.03
P_2O_5	0.0	0.2	0.02
MgO	0.0	0.0	0.0
K_2O	0.0	0.31	0.03
Ag_2O	0.0	0.04	0.05

Brunauer-Emmett-Teller (BET) analysis.

The surface characteristics of the precursors and composite catalyst were quantitatively ascertained using the Brunauer-Emmett-Teller (BET) analysis. The surface area, pore diameter and pore volume determined from the analysis are displayed in table 2 below.

The textural properties of the precursors and the resulting composite catalyst highlight a strategic structural evolution suitable for high-efficiency catalysis. The anthill clay (AC) precursor exhibits the highest specific surface area at **314.2 m^2/g**, confirming its role as a superior aluminosilicate scaffold with an inherent capacity for high active-site dispersion [5]; [22]. Following the integration of calcium carbide residue (CCR) and the 1.5 M zinc nitrate dopant, the surface area of the composite catalyst settles at **226.9 m^2/g**. This reduction, alongside a decrease in pore volume from **0.28 cc/g** to **0.2 cc/g**, indicates that the metal oxides successfully occupied the AC pore network during the 750 °C calcination phase [1].

Critically, all materials maintain a consistent pore diameter within the **2.8–2.9 nm** range, identifying the system as distinctly **mesoporous**. This pore size is ideal for biodiesel production as it allows for the unhindered diffusion of bulky triglyceride molecules to the active sites within the catalyst matrix, thereby minimizing mass transfer resistance [13]. The final composite combines a robust surface area with an optimized mesoporous architecture, ensuring the necessary site accessibility to facilitate the peak yields observed in the production tests [7]; [16].

Table 2: Surface characteristics of precursors and composite catalyst

Parameter	CCR	AC	Composite catalyst
Surface area (m^2/g)	221.7	314.2	226.9
Pore diameter (nm)	2.9	2.8	2.9
Pore volume (cc/g)	0.20	0.28	0.2

Characterization of the oil feedstock (PKO)

The physicochemical properties of the Palm Kernel Oil (PKO) as presented in Table 3 indicate that while the oil is a viable feedstock for biodiesel production, its high acidity necessitates the use of a specialized catalytic system. The Acid Value of 7.3 mgKOH/g and a corresponding Free Fatty Acid (FFA) content of 3.7% exceed

ISSN 2278-2540 | DOI: 10.51583/IJLTEMAS | Volume XV, Issue V, May 2026

the typical 1% threshold for simple base-catalyzed transesterification. This level of acidity confirms the importance of using the ZnO-doped bifunctional catalyst synthesized in this study, as the Lewis acidic sites provided by the ZnO are essential for the simultaneous esterification of FFAs and transesterification of triglycerides to prevent soap formation [2].

The structural and energy characteristics of the PKO are further defined by its Saponification Value of 234.2 mgKOH/g and Average Molecular Weight of 742 g/mol. These high values suggest a prevalence of short-to-medium chain fatty acids, which are beneficial for producing biodiesel with low viscosity and high volatility. Furthermore, the Iodine Value of 19 mg I_2/100g is notably low, indicating a high degree of saturation. This is a positive indicator for the resulting biofuel's oxidative stability, suggesting it will be less prone to rancidity or sludge formation during long-term storage [13]; [19].

Physical and purity parameters such as the Density (0.90 g/cm³) and Viscosity (5.2 m²/s) align with standard profiles for tropical vegetable oils. However, the Moisture Content of 1.09% and Peroxide Value of 16 mEq/kg suggest a slight degree of primary oxidation and water presence, which can lead to competitive side reactions. Despite these impurities, the overall profile confirms that the PKO is an ideal candidate for conversion into high-quality biodiesel when processed with an optimized, thermally activated bifunctional catalyst [1].

Table 3: Physiochemical properties of PKO

Property	**Value**
Density (g/cm^3)	0.90
Average molecular weight (g/mol)	742
Peroxide value (mEq/kg)	16
Acid value (mgKOH/g oil)	7.3
Free Fatty Acid (%)	3.7
Saponification value (mgKOH/g oil)	234.2
Viscosity @ 40^{o}C, 30.0 RPM & 22% (m^2/s)	5.2
Moisture content (%)	1.09
Iodine value (mg I_2/100g oil)	19

Biodiesel production

Table 4: Results of biodiesel production for effect of calcination temperature on catalysts functionality

Catalyst	Catalyst composition (CCR:AC)	Calcination temperature (^{o}C)	Reaction temperature (^{o}C)	Reaction time (mins)	Methanol-to-oil ratio (-)	Catalyst loading (wt.%)	Biodiesel yield (%)
A1	1:4	650	65	90	9	3	64.36
A2	1:4	750	65	90	9	3	70.58
A3	1:4	850	65	90	9	3	68.59
B1	2:3	650	65	90	9	3	71.44
B2	2:3	750	65	90	9	3	76.23
B3	2:3	850	65	90	9	3	74.81
C1	1:1	650	65	90	9	3	75.34

ISSN 2278-2540 | DOI: 10.51583/IJLTEMAS | Volume XV, Issue V, May 2026

C2	1:1	750	65	90	9	3	77.53
C3	1:1	850	65	90	9	3	76.86
D1	3:2	650	65	90	9	3	80.23
D2	3:2	750	65	90	9	3	92.73
D3	3:2	850	65	90	9	3	87.45
E1	4:1	650	65	90	9	3	79.32
E2	4:1	750	65	90	9	3	88.74
E3	4:1	850	65	90	9	3	85.23

Biodiesel production

The data in Table 4 illustrates a distinct parabolic relationship between calcination temperature and catalytic activity across all catalyst groups (A through E). While the catalyst composition (the ratio of CCR to AC) sets the baseline for potential yield, the thermal treatment—specifically the choice of 750 °C—acts as the critical "activation switch" for achieving maximum efficiency.

Thermal Activation and the 750 °C Optimum

Across every series, the biodiesel yield peaks at a calcination temperature of 750 °C (e.g., A2, B2, C2, D2, and E2). This temperature appears to be the "sweet spot" for several physicochemical transformations. At 750 °C, the precursors undergo optimal decomposition and phase transformation—specifically the conversion of calcium carbonates from CCR into active CaO and the integration of the zinc dopant into the metal oxide matrix.

This creates a high density of active basic sites and a well-developed pore structure that facilitates the diffusion of large triglyceride molecules. Recent studies confirm that this temperature range is ideal for maximizing crystallinity and surface basicity in heterogeneous calcium-based catalysts [14].

The Decline at 850 °C: Sintering and Structural Degradation

A consistent decline in yield is observed when the calcination temperature is increased further to 850 °C (e.g., A3, B3, C3, D3, and E3). For instance, in the D-series, the yield drops from its peak of 92.73% (D2) to 87.45% (D3). This "thermal over-treatment" typically leads to a phenomenon known as sintering, where small catalyst particles fuse together.

This fusion reduces the total surface area and causes "pore collapse," effectively burying active sites that were previously accessible for the reaction. Modern characterization research highlights that excessively high temperatures can also lead to the formation of less active mixed-metal oxides or solid-state reactions that neutralize the basic sites necessary for methanol activation [13].

Synergistic Effect of Composition and Temperature

The table also reveals that the effect of temperature is more pronounced as the CCR (Calcium) content increases. In Group A (1:4 ratio), the jump from 650 °C to 750 °C only improves the yield by about 6%. However, in Group D (3:2 ratio), the same 100 °C increase results in a massive 12.5% surge in yield (from 80.23% to 92.73%).

This suggests that a higher concentration of the basic precursor requires this specific thermal energy to fully unlock its bifunctional potential. The combination of high CCR content and 750 °C calcination provides the most effective acidity/basicity balance for simultaneous esterification and transesterification [20].

ISSN 2278-2540 | DOI: 10.51583/IJLTEMAS | Volume XV, Issue V, May 2026

Influence of Calcination Temperature on Catalyst Activity and Biodiesel Yield

The biodiesel yield profiles demonstrate that **750 °C** is the optimal calcination temperature for maximum catalytic efficiency, yielding a peak of **92.73%**. This temperature acts as a critical threshold, providing sufficient thermal energy to fully activate the **CaO** and **ZnO** species while preserving the catalyst's porous structure.

Lower temperatures, such as **650 °C**, result in "under-calcination," where incomplete precursor decomposition leads to a deficit of active basic sites and lower yields (e.g., 80.23%). Conversely, increasing the temperature to **850 °C** triggers thermal sintering and pore collapse, reducing the accessible surface area and causing the yield to drop to **87.45%**.

The superior performance at **750 °C** ensures high site accessibility and stable crystallinity, consistent with recent findings that identify this window as the "activation sweet spot" for bifunctional catalysts [13]; [16].

In conclusion, calcination temperature significantly influenced catalyst structure and catalytic activity. Moderate calcination temperatures promoted decomposition of precursor species and formation of active CaO phases, while excessive temperatures may have induced particle sintering and pore collapse, resulting in reduced surface area and catalytic performance.

Reaction kinetics

Reaction kinetics plays an important role in biodiesel production because it determines the rate at which triglycerides are converted into fatty acid methyl esters during the transesterification process. The reaction rate is influenced by several factors, including reaction temperature, reaction time, methanol-to-oil ratio, catalyst loading, and agitation speed. In heterogeneous catalysis, the availability of active basic sites, catalyst surface area, pore structure, and mass transfer between the reactants and catalyst surface also significantly affect the conversion efficiency. In this study, the improved biodiesel yield observed at the optimum calcination temperature may be attributed to enhanced catalyst crystallinity, increased formation of active basic sites, and improved dispersion of ZnO species on the catalyst surface. However, excessively high calcination temperatures may lead to particle agglomeration and pore collapse, thereby reducing catalytic activity and biodiesel yield. Although detailed kinetic modeling was beyond the scope of this work, the findings suggest that calcination temperature strongly influences the catalytic behavior and transesterification efficiency of the ZnO-doped CaO/anthill clay catalyst.

Catalyst activation mechanism

The catalytic mechanism likely involves the generation of strong basic sites from CaO and ZnO species, which facilitate methoxide ion formation during transesterification. The anthill clay support improves catalyst dispersion, thermal stability, and surface area, thereby enhancing accessibility of active sites.

Catalyst reusability studies

In the first run, the biodiesel yield was 92.73 %. The second, third and fourth runs produced yields of 86.93 %, 79.03 % and 76.54 %, respectively. The fifth and sixth runs recorded biodiesel yields of 70.14 %, and 65.04 % respectively, as illustrated in Figure 9 below. A steady decline in biodiesel yield was observed with increasing reuse cycles, amounting to an overall reduction of about 27.69 % between the first and sixth runs.

This decrease in performance may be attributed to the gradual occupation of the catalyst’s active sites by unreacted triglycerides, which reduces the availability of active sites and consequently lowers catalytic efficiency [23]

ISSN 2278-2540 | DOI: 10.51583/IJLTEMAS | Volume XV, Issue V, May 2026

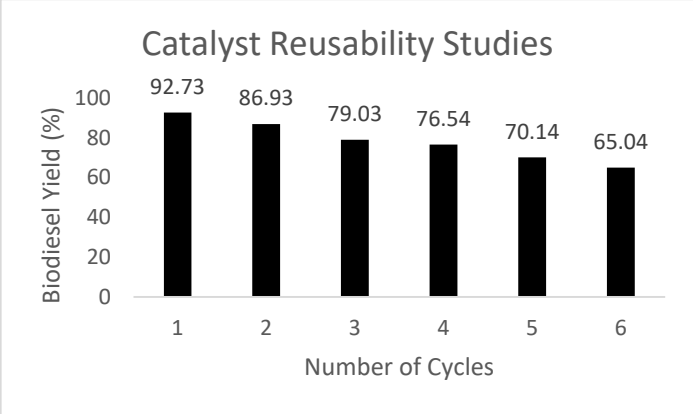

Figure 9: Catalyst reusability studies results

Characterization of the produced biodiesel

The physicochemical properties of the produced biodiesel, as detailed in Table 5, demonstrate that the fuel is of high quality and fully complies with the international ASTM D6751 and EN 14214 standards. A standout feature of this fuel is its Cetane number of 67.44, which significantly exceeds the minimum requirements of 47 and 51, respectively. This high value indicates superior ignition quality, which leads to smoother engine performance and reduced noise during combustion. Furthermore, the Higher Heating Value (40.64 MJ/kg) confirms that the biodiesel possesses an energy content comparable to conventional petroleum diesel, ensuring efficient power generation [2].

The safety and flow characteristics of the fuel are also well within the optimized range for engine use. The Flash point of 179 °C is substantially higher than the required minimum of 130 °C, making the biodiesel exceptionally safe for long-term storage and transportation. Additionally, the Viscosity at 40 °C (3.6 mPa.s) falls perfectly within the standard limits, which is critical for ensuring proper fuel atomization and preventing wear on the fuel injection pump. The cold flow properties, represented by a Pour point of -5 °C and a Cloud point of -6 °C, suggest that the fuel will remain liquid and functional in moderately cold climates [1]; [19].

Finally, the chemical stability and purity of the biodiesel are confirmed by its low acidity and saturation levels. The Acid value (0.266 mgKOH/g) and Free Fatty Acid content (0.133%) are well below the corrosive thresholds, protecting engine components from damage. Moreover, the low Iodine value (23.5 g I_2/100g) suggests a low level of unsaturation, which significantly improves the fuel's oxidative stability and prevents the formation of sludge during storage. Overall, these properties validate the effectiveness of the ZnO-doped CaO/Anthill clay catalyst in producing a high-grade, stable, and environmentally friendly biofuel [13].

Table 5: Properties of biodiesel

Properties	**Biodiesel**	**ASTM D6751**	**EN 14214**
Colour	Golden yellow	Not specified	Not specified
Physical state at room temperature	Liquid	Not specified	Not specified
Density (g/cm^3)	0.863	Not specified	Not specified
Acid value (mgKOH/g)	0.266	<0.5	<0.5
Free fatty acid (%)	0.133	Not specified	Not specified
Saponification value (mgKOH/g)	206.44	Not specified	Not specified
Iodine value (I_2/100g)	23 .5	Not specified	<120
Viscosity @ 40 ^{o}C (mPa.s)	3.6	1.9 to 6.0	3.5 to 5.0

ISSN 2278-2540 | DOI: 10.51583/IJLTEMAS | Volume XV, Issue V, May 2026

Pour point (^oC)	-5	<0	<0
Flash point (^oC)	179	>130	>120
Cloud point (^oC)	-6	Not specified	Not specified
Cetane number	67.44	≥47	≥51
Higher heating value	40.64	Not specified	≥35
Aniline point	81	Not specified	Not specified

Economic feasibility and scalability of catalyst production

The catalyst precursors used in this study are naturally occurring inexpensive and abundantly available waste-derived materials (anthill clay and calcium carbide residue), making the catalyst economically attractive for large-scale biodiesel production. The synthesis procedure, involving calcination and impregnation, is relatively simple and adaptable to industrial-scale operations. Furthermore, the low ZnO loading reduces overall catalyst production cost while enhancing catalytic activity. However, detailed techno-economic analysis and pilot-scale validation were beyond the scope of this study and should be investigated in future work.

Environmental impact and energy consumption

The use of waste-derived catalyst materials contributes to sustainable waste valorization and reduces environmental impact. In addition, heterogeneous catalysis minimizes soap formation and wastewater generation during biodiesel purification. Nevertheless, catalyst calcination remains energy-intensive, and future studies should focus on reducing thermal energy requirements for sustainable large-scale production.

CONCLUSION

This study successfully achieved its primary goal of synthesizing a high-performance ZnO-doped CaO/Anthill clay composite using calcium carbide residue and anthill clay as sustainable precursors. By evaluating a thermal range from 650 °C to 850 °C, it was determined that the calcination temperature is the critical factor in balancing chemical activation with structural stability. The research identified 750 °C as the optimal temperature, as it successfully maximized the density of active sites while preventing the structural degradation and sintering observed at higher temperatures. Testing the catalyst's effectiveness on palm kernel oil confirmed its high efficiency, reaching a peak biodiesel yield of 92.73% with catalyst reusability evaluation giving an overall reduction of 27.69 % in biodiesel yield across 6 cycles. These findings demonstrate that utilizing waste materials provides a cost-effective and environmentally friendly pathway for biodiesel production. The produced biodiesel properties aligned with ASTM D6571 and EN 14214 standards upon characterization. This study contributes to the promotion of renewable and sustainable energy.

ACKNOWLEDGEMENTS

The authors wish to acknowledge the Petroleum Technology Development Fund (PTDF) for supporting thi s study, through the PTDF Professorial Chair on Renewable Energy in the Department of Chemical Engineering, University of Benin, Nigeria.

REFERENCES

1. Ajala, E. O., Ajala, M. A., Afolabi, F. D., Ajala, J. O., Opawoye, S., & Ariyoosu, D. A. (2024). Waste-ram-fat as a Feedstock for Biodiesel Production using Heterogeneous Catalyst of Kaolinite-clay Impregnated Calcium-oxide from Chicken Eggshell. *Nigerian Journal of Technological Development*, *21*(4), 168–179. https://doi.org/DOI:10.63746/njtd.v21i4.3104
2. Akpan, I., Edeh, I., & Uyigue, L. (2026). *The Influence of bifunctional Heterogeneous Catalyst on Biodiesel Production from Oleochemicals*. *9*(10), 1864–1870. https://doi.org/10.64388/IREV9I10-

ISSN 2278-2540 | DOI: 10.51583/IJLTEMAS | Volume XV, Issue V, May 2026

1716580
3. Al-bayati, B. B., Özdemir, O. K., Khudhur, A. G., Özdemir, J. H., Hantosh, A. A., Al-sheikh, F., Özdemir, O. K., Khudhur, A. G., & Özdemir, J. H. (2025). Mitigation of SrO catalyst leaching and recyclability in biodiesel transesterification : comprehensive parameter optimization and characterization via FTIR spectroscopy. *Biofuels*, 1–19. https://doi.org/10.1080/17597269.2025.2560708
4. Al-Sakkari, E. G., El-Sheltawy, S. T., Attia, N. K., & Mostafa, S. R. (2017). Kinetic study of soybean oil methanolysis using cement kiln dust as a heterogeneous catalyst for biodiesel production. *Applied Catalysis B: Environmental*, *206*, 146–157. https://doi.org/10.1016/j.apcatb.2017.01.008
5. Babatunde, E. O., & Mekuto, L. (2025). Optimization of Biodiesel Production from Used Vegetable Oil using Functionalized Catalyst derived from Anthill. *Ngerian Journal of Technological Development*, *22*(1), 1–9.
6. Fattah, R. I. M., Ong, H. C., Mahlia, T. M. I., Mofijur, M., Silitonga, A. S., Rahman, A. S. M., & Ahmad, A. (2020). State of the Art of Catalysts for Biodiesel Production. *Frontiers in Energy Research*, *8*, 101. https://doi.org/10.3389/fenrg.2020.00101
7. Hughes, J., Hart, A., Das, B., & Wood, J. (2026). Advances in the Application of Low-Cost , Natural Materials , and Waste-Derived Catalysts for Catalytic Upgrading of Plastic and Biomass Pyrolysis Oil. *Energy Fuels*, *40*(5), 2338−2371. https://doi.org/10.1021/acs.energyfuels.5c05623
8. Ifeanyi-Nze, F. O., Omiyale, C. O., Okonkwo, I. U., Chukwu, J. C., Nwankwor, Maryjane, C., Onabanjo, A. O., Adoga, S. O., Chukwu, J. O., Chukwurah, K. F., Ebikemiyen, M., Okon, G. U., Adeleke, O. J., & Tajudeen, K. A. (2023). Biodiesel Synthesis from Waste Vegetable Oil Utilizing Eggshell Ash as an Innovative Heterogeneous Catalyst. *Archives of Advanced Engineering Science*, 1–18. https://doi.org/10.47852/bonviewAAES32021761
9. Krishnan, S. G., Pua, F., & Lim, H. (2022). Synthesis of Magnetic Base Catalyst from Industrial Waste for Transesterification of Palm Oil. *Bulletin of Chemical Reaction Engineering & Catalysis*, *17*(1), 53–64. https://doi.org/10.9767/bcrec.17.1.12412.53-64 10 Macheli, L., Leteba, G. M., Jewell, L. L., George, S. L., & Lang, I. (2026). Enhancing waste eggshell-derived CaO catalysts for biodiesel production through synergistic oxide modification : a comprehensive catalytic and kinetic study. *RSC Advances*, *16*, 5990–6001. https://doi.org/10.1039/D5RA06382E
10. Makarevičienė, V., Gaidė, I., & Sendžikienė, E. (2025). Heterogeneous Catalysts from Food Waste for Biodiesel Synthesis — A Comprehensive Review. *Catalysts*, *15*(10), 957. https://doi.org/doi.org/10.3390/catal15100957
11. Malabadi, R. B., Kolkar, K. P., & Chalannavar, R. K. (2023). Biodiesel production : An updated review of evidence. *International Journal of Biological and Pharmaceutical Sciences Archive*, *06*(02), 110–133.
12. Mohammed, J., Aremu, M. O., & Usman, A. (2026). Synthesis and characterization of biodiesel from black date (Canarium schweinfurtii) seed kernel oil in the presence of green-synthesized Cu-Mn / TiO 2 nanocatalyst using central composite design approach. *Recent Advances in Natural Sciences 4 227*, *4*, 227. https://doi.org/10.61298/rans.2026.4.1.227
13. Nurdina, R. A., Kamiya, Y., Hatmanto, A. D., & Pambudi, F. I. (2025). Ultrasonic-Assisted Transesterification of Tripalmitin Using Limestone-Derived CaO Catalyst. *Bulletin of Chemical Reaction Engineering & Catalysis*, *20*(4), 672–682. https://doi.org/10.9767/bcrec.20456
14. Obahiagbon, K., Offiah, U., & Ahonkhai, D. O. (2025). Optimized Biodiesel Production from Palm Kernel Oil Using a Bifunctional Catalyst from Cocoa Pod and Pig Bone. *Petroleum Technology Development Journal*, *15*(2), 1–15.
15. Ogunkunle, O., & Olusanya, M. O. (2026). Biodiesel synthesis from Blighia sapida seed oil : comparative modelling via RSM and ANFIS – PSO hybrid optimization. *Frontiers in Energy Research*, *14*, 1783127. https://doi.org/10.3389/fenrg.2026.1783127
16. Okhonmina, J. O., Obahiagbon, K., & Oyedoh, E. A. (2026). Optimum Biodiesel Production from Palm Kernel Oil Using Heterogeneous Catalyst from Carbide Slag and Termite Hill Clay. *International Journal of Research and Innovation in Applied Science (IJRIAS)*, *11*(3), 520–543. https://doi.org/10.51584/IJRIAS
17. Singh, D., Singh, K., Jadeja, Y., Menon, S. V, Singh, P., Ibrahim, S. M., & Singh, M. (2025). Magnetic nano-sized solid acid catalyst bearing sulfonic acid groups for biodiesel synthesis and oxidation of sulfides. *Scientific Reports*, *15*(1), 1397. https://doi.org/https://doi.org/10.1038/s41598-024-84494-x
18. Uzuegbu, J. N., Babayemi, A. K., Ezeugo, J. O., & Umeuzuegbu., J. C. (2026). Biodiesel Production from

ISSN 2278-2540 | DOI: 10.51583/IJLTEMAS | Volume XV, Issue V, May 2026

Jatropha Seeds Using a Waste-Derived Periwinkle Shell Heterogeneous Catalyst. *Chemical Science International Journal*, *35*(2), 19–34.

19. Widayat, W., Hadiyanto, H., Hargono, H., Abdullah, A., Syalom, M. N., Setiawan, A., & Philia, J. (2025). Optimization of biodiesel production from candlenut oil via simultaneous reaction using a bifunctional CeO 2 . CaO catalyst. *International Journal of Renewable Energy Development*, *14*(6), 1273–1284.
20. Yusuff, A. S., Adeniyi, O. D., Olutoye, M., & Akpan, U. G. (2018). The potential of composite anthill-waste chicken eggshell as heterogeneous catalyst in biodiesel production. *Petroleum and Coal*, *60*(1), 58–70.
21. Yusuff, A. S., & Adesina., O. A. (2020). Biodiesel Synthesis from Palm Olein Oil using Anthill as Catalyst. *Journal of Chemical Technology & Metallurgy*, *55*(2).
22. Yusuff, A. S., Gbadamosi, A. O., & Popoola, L. T. (2021). Journal of Environmental Chemical Engineering Biodiesel production from transesterified waste cooking oil by zinc-modified anthill catalyst : Parametric optimization and biodiesel properties improvement. *Journal of Environmental Chemical Engineering*, *9*(2), 104955. https://doi.org/10.1016/j.jece.2020.104955